

Influence of Nonuniform Laser Intensities on Ablatively Accelerated Targets

Mark H. Emery, Joseph H. Orens,^(a) John H. Gardner, and Jay P. Boris
Laboratory for Computational Physics, Naval Research Laboratory, Washington, D. C. 20375
 (Received 28 May 1981)

The effect of a nonuniform laser beam on the ablative acceleration of thin foils is investigated by using the FAST2D laser-shell simulation code. The results show that laser nonuniformities with scale lengths greater than the distance from the ablation surface to the critical surface would have a severe impact on drive pressure symmetry and hence on pellet gain.

PACS numbers: 52.50.Jm, 52.55.Mg

In laser fusion, spherical layered pellets are imploded through laser-induced ablation of the outer surface. In order to achieve the densities and temperatures required for thermonuclear fusion, this inward acceleration must be very symmetric over the surface of the pellet. For laser fusion to be practical, the laser energy must be efficiently coupled to the pellet. Implosion symmetry and energy efficiency may be conflicting requirements.

Experiments and theory at the Naval Research Laboratory¹ and elsewhere² indicate that the most efficient laser energy coupling occurs at relatively low irradiances (from 10^{12} to 10^{14} W/cm²). These low irradiances require thin-shelled pellets³ (of thickness ΔR) to be accelerated over large distances (R) such that $R/\Delta R \geq 10$. This places severe requirements on ablation pressure uniformity ($\Delta p/p \leq 1\%$) if high gain is to be achieved.⁴ One of the major causes of ablation pressure nonuniformity is nonuniformity of the laser beam intensity. The problem we address in this Letter is the effect of nonuniform laser intensities on the ablation pressure of thin planar targets as a function of laser intensity and scale length of the inhomogeneity.

The laser energy is deposited at the critical surface, a distance D_{ac} from the ablation surface. The scale length of the inhomogeneity in laser intensity is λ_l . If $D_{ac} \gg \lambda_l$, then lateral energy flow should smooth out the inhomogeneity before it reaches the ablation surface.^{4,5} If $D_{ac} \ll \lambda_l$, then the inhomogeneity should imprint itself on the target and the variation in ablation pressure should be of the same order as the variation in laser intensity. This inhomogeneity in ablation pressure will, in turn, affect the target velocity and acceleration profiles.

We model the effect of an inhomogeneous laser beam on a thin (15 μm thick) plastic (CH) foil with the FAST2D⁶ laser-shell simulation code.

This is a fully two-dimensional Cartesian code with a sliding rezoned Eulerian grid. It solves the ideal hydrodynamic equations using the flux-corrected transport⁷ algorithms with a two-dimensional, classical ($T^{5/2}$) plasma thermal conduction routine. FAST2D compares well with experimental data on ablation pressure, hydrodynamic efficiency, and target velocities,⁸ and with fluid velocity profiles.⁹

Laser beam profiles are typically Gaussian with inhomogeneities manifesting themselves by a reduced intensity in the center of the beam. We invoke the periodicity of the code and model only the peak-to-peak variation in intensity. Three different average laser intensities, $\langle I \rangle = 5 \times 10^{12}$, 1×10^{13} , and 2×10^{13} W/cm², are used with the scale length of the inhomogeneity ranging between 100 and 600 μm . For all the results presented here the variation in intensity is 73%

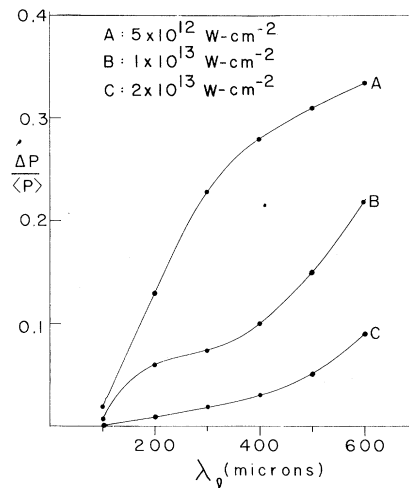


FIG. 1. The variation in ablation pressure ($\Delta p/\langle p \rangle$) as a function of the scale length of the inhomogeneity (λ_l) for three different average laser intensities ($\langle I \rangle = 5.0 \times 10^{12}$, 1.0×10^{13} , and 2.0×10^{13} W/cm²).

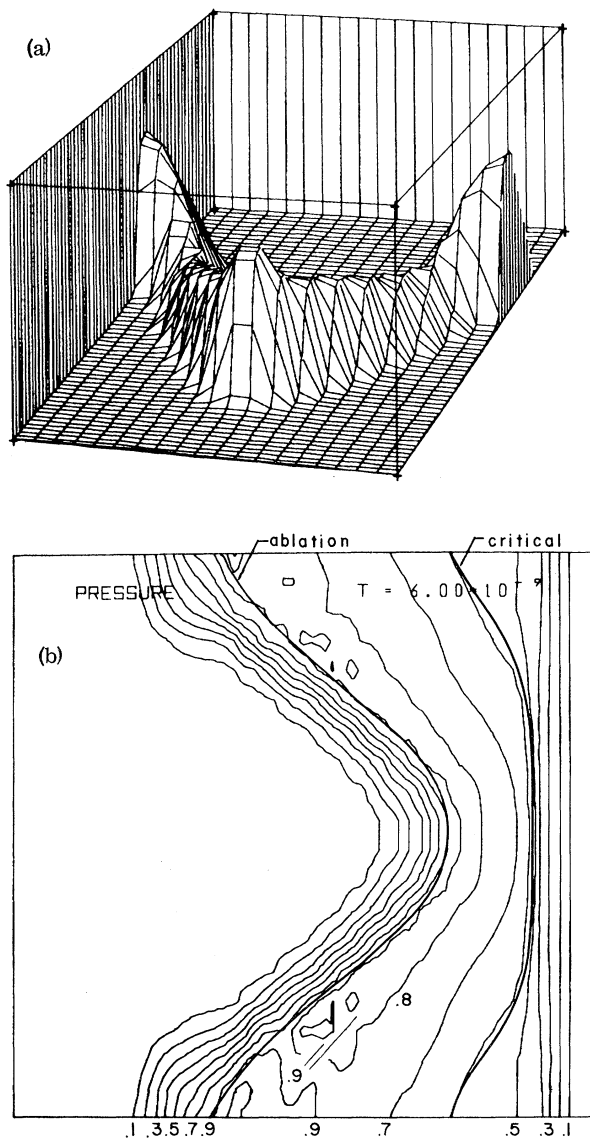


FIG. 2. (a) The perspective density plot for $\langle I \rangle = 1.0 \times 10^{13} \text{ W/cm}^2$ and $\lambda_i = 600 \mu\text{m}$ after 6 nsec. The foil is severely distorted and beginning to buckle. (b) Pressure contours for $\langle I \rangle = 1.0 \times 10^{13} \text{ W/cm}^2$ and $\lambda_i = 600 \mu\text{m}$. The lines are contours of constant pressure in 0.10 increments of the maximum pressure ($p_{\text{max}} = 2.88 \text{ Mbar}$). The critical and ablation surfaces are also indicated.

($\Delta I / \langle I \rangle = 0.73$, $\Delta I = I_{\text{max}} - I_{\text{min}}$) and the laser wavelength is $1.06 \mu\text{m}$.

Figure 1 shows the variation in the ablation pressure as a function of the scale length of the inhomogeneity for the three intensities after 3 nsec. Note that the large-scale-length variation ($\lambda_i = 600 \mu\text{m}$) severely impacts the target for all three intensities. For case A, $\langle I \rangle = 5.0 \times 10^{12} \text{ W/}$

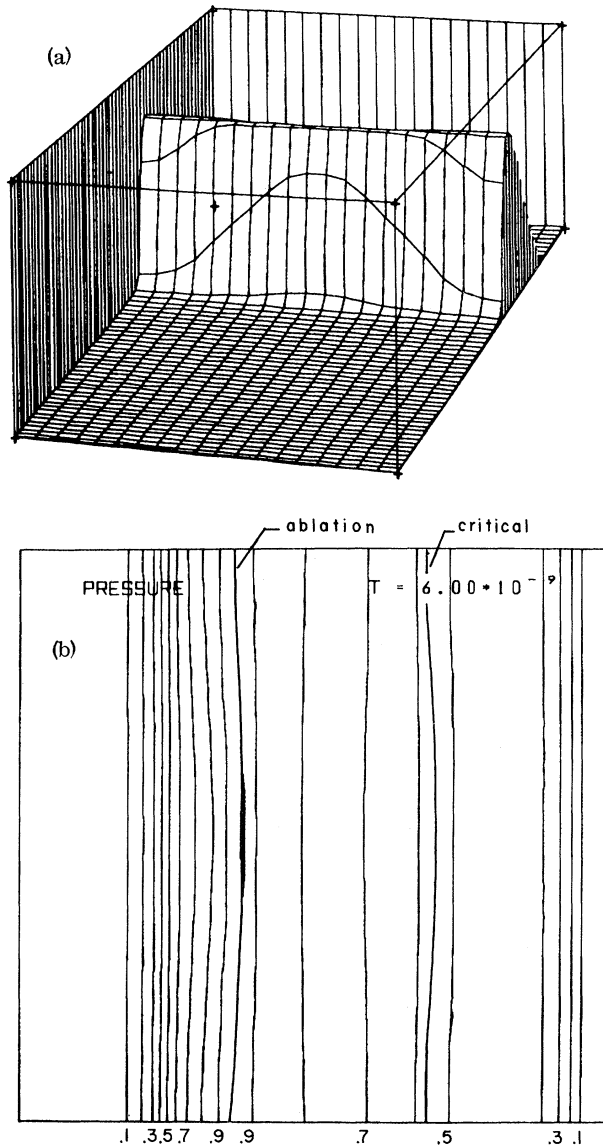


FIG. 3. (a) The perspective density plot for $\langle I \rangle = 1.0 \times 10^{13} \text{ W/cm}^2$ and $\lambda_i = 100 \mu\text{m}$ after 6 nsec. At this short scale length, very little distortion is observed. (b) Pressure contours for $\langle I \rangle = 1.0 \times 10^{13} \text{ W/cm}^2$ and $\lambda_i = 100 \mu\text{m}$ ($p_{\text{max}} = 2.63 \text{ Mbar}$).

cm^2 , lateral energy flow has no significant impact for scale lengths greater than $100 \mu\text{m}$ whereas for case C, $\langle I \rangle = 2.0 \times 10^{13} \text{ W/cm}^2$, lateral flow gives rise to only a 5% pressure variation for $\lambda_i = 500 \mu\text{m}$.

The average ablation pressures and the average velocities of the foils were approximately constant for each intensity with little dependence on the asymmetry scale length. These values are case A: $\langle p_{\text{ab}} \rangle = 1.68 \text{ Mbar}$, $\langle V \rangle = 2.14 \times 10^6 \text{ cm/s}$;

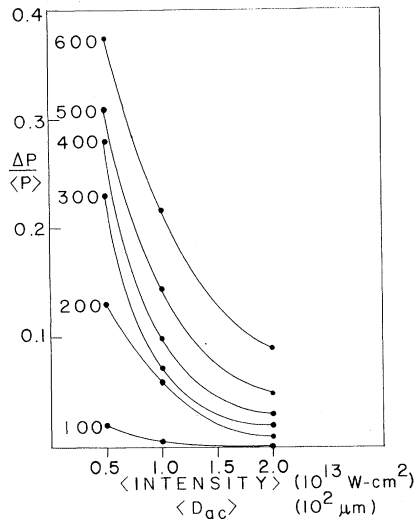


FIG. 4. The variation in ablation pressure ($\Delta p/\langle p \rangle$) for all six scale lengths plotted as a function of the average laser intensity ($\langle I \rangle$) and as a function of the average distance from the ablation surface to the critical surface ($\langle D_{ac} \rangle$).

case B: $\langle p_{ab} \rangle = 2.64$ Mbar, $\langle V \rangle = 4.76 \times 10^6$ cm/s; and case C: $\langle p_{ab} \rangle = 3.85$ Mbar, $\langle V \rangle = 7.31 \times 10^6$ cm/s.

A perspective plot of the density at 6 nsec for case B, $\lambda_l = 600 \mu\text{m}$, is shown in Fig. 2(a). As can be seen, the ablation rate variation follows the laser intensity variation and the foil becomes severely distorted and is beginning to buckle. Figure 2(b) illustrates the pressure contours at the same time. Note the pockets of very high pressure at the "edges" of the ablation surface. These are, of course, the regions of highest laser intensity.

The density plot and pressure contours for case B, $\lambda_l = 100 \mu\text{m}$, are given in Figs. 3(a) and 3(b). Here there is negligible distortion of the foil and the ablation surface is essentially equivalent to a contour surface. Lateral energy flow has provided enough smoothing to produce only a 0.5% variation in the ablation pressure.

The numerical results are summarized in Fig. 4, where the variation in ablation pressure is plotted as a function of the average laser intensity for all six scale lengths. This is equivalent to plotting the variation in ablation pressure as a function of the average distance between the ablation surface and the critical surface as indicated on the graph. These results are in very good agreement with the experimental results obtained at the Naval Research Laboratory¹⁰ as shown in

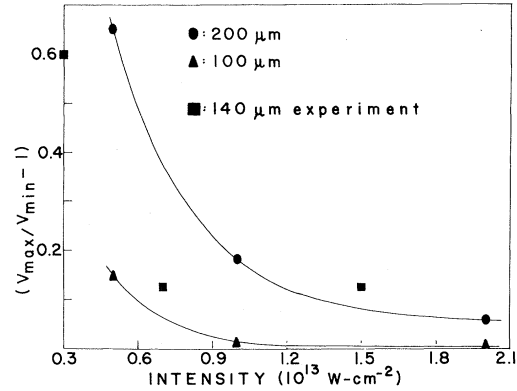


FIG. 5. Comparison of the numerical results for the 100- and 200- μm scale lengths with a 140- μm -scale-length experimental result (Ref. 10).

Fig. 5 where we compare the foil velocity non-uniformity ($V_{max}/V_{min} - 1$) for the 100- and 200- μm asymmetries to the experimental results for a 140- μm asymmetry with $I_{max}/I_{min} \approx 2$. We obtain slightly better smoothing at the higher irradiances which is probably due to our slightly thicker target.¹⁰

In summary, we have shown that lateral energy flow in the form of transverse thermal conduction does tend to smooth the effects of laser beam nonuniformities. The degree of smoothing is directly related to the distance from the ablation surface to the critical surface.¹¹ To smooth non-uniformities to the extent that the ablation pressure variation is less than 1% requires that $D_{ac} \sim O(\lambda_l)$.

These results indicate that laser asymmetries must be considered in the design of a reactor-size laser fusion system. With use of a many-beam system with severe overlap, each beam would have a spot size on the order of the target radius (2–5 mm), giving rise to intensity variations of the same order. To smooth intensity variations of this order by employing very high irradiances increases the possibility of plasma instabilities and poor absorption. One-dimensional numerical results¹² indicate that the distance between the ablation and critical surfaces scales as $D_{ac} \propto I/\omega^3$, where ω is the frequency of the laser light. It would seem that the most likely means to increase the distance from the ablation surface to the critical surface is to reduce the frequency of the laser light.^{11,13} Although short-wavelength lasers appear to have some advantages¹⁴ (higher absorption and ablation rates and reduced hot-electron temperatures), these ad-

vantages may be eclipsed by the critical problem of laser asymmetries.

The authors gratefully acknowledge the helpful suggestions and conversations with S. E. Bodner, J. Grun, M. J. Herbst, S. P. Obenschain, and B. H. Ripin at the Naval Research Laboratory. This research was supported by the U. S. Department of Energy.

^(a)Present address: Berkeley Research Associates, Springfield, Va. 22150.

¹B. H. Ripin *et al.*, Phys. Fluids **23**, 1012 (1980).

²J. P. Anthes *et al.*, Appl. Phys. Lett. **34**, 841 (1979).

³Y. V. Afanasév *et al.*, Pis'ma Zh. Eksp. Teor. Fiz. **21**, 150 (1975) [JETP Lett. **21**, 68 (1975)].

⁴J. Nuckolls *et al.*, Nature (London) **239**, 139 (1972).

⁵W. C. Mead and J. D. Lindl, Lawrence Livermore Laboratory Report No. UCRL-78459, 1976 (unpublished), and Bull. Am. Phys. Soc. **21**, 1102 (1976).

⁶J. P. Boris, Naval Research Laboratory Memorandum Report No. 3427, 1976 (unpublished); J. P. Boris, Comments Plasma Phys. Controlled Fusion **3**, 1 (1977).

⁷J. P. Boris and D. L. Book, Methods Comput. Phys. **16**, 85 (1976).

⁸Naval Research Laboratory Laser-Plasma Interaction Group, Naval Research Laboratory Memorandum Report No. 4369, 1980 (unpublished).

⁹M. Herbst *et al.*, Bull. Am. Phys. Soc. **26**, 1024 (1981).

¹⁰S. P. Obenschain *et al.*, Phys. Rev. Lett. **46**, 1402 (1981).

¹¹Mark H. Emery *et al.*, Bull. Am. Phys. Soc. **25**, 947 (1980), and Naval Research Laboratory Memorandum Report No. 4500, 1981 (unpublished).

¹²J. H. Gardner and S. Bodner, Phys. Rev. Lett. **47**, 1137 (1981).

¹³S. Bodner, Naval Research Laboratory Memorandum Report No. 4453, 1981 (unpublished).

¹⁴C. E. Max, Bull. Am. Phys. Soc. **25**, 992 (1980); E. Fabre, Bull. Am. Phys. Soc. **25**, 992 (1980); D. C. Slater, Bull. Am. Phys. Soc. **25**, 992 (1980).

Absence of Fast Electrons in Laser-Irradiated Gas-Jet Targets

J. A. Tarvin, F. J. Mayer, D. C. Slater, Gar. E. Busch, G. Charatis,
T. R. Pattinson, R. J. Schroeder, and D. Sullivan
KMS Fusion, Inc., Ann Arbor, Michigan 48106

and

D. L. Matthews

Lawrence Livermore National Laboratory, Livermore, California 94550

(Received 2 November 1981)

The x-ray spectrum emitted by a gas jet irradiated at 10^{16} W/cm² has been measured for laser wavelengths of 1.05 and 0.53 μ m. The flux of hard x rays ($h\nu \geq 10$ keV) emitted by a gas jet is less than 0.3% of that emitted by a glass target irradiated at the same intensity. This low flux implies that less than 0.1% of the incident energy is used to heat electrons to energies greater than 10 keV.

PACS numbers: 52.25.Ps, 52.25.Fi, 52.40.Db

The aim of laser-fusion studies is to compress deuterium-tritium fuel to high density and then heat it to produce a thermonuclear reaction. The production of electrons with energies greater than 10 keV in laser-irradiated plasmas lowers the efficiency of the thermonuclear burn by limiting fuel density. The fast electrons heat the interior of an imploding target prematurely, making the fuel more difficult to compress; and they transport energy from the absorption region to the low-density expanding corona, reducing the efficiency with which absorbed energy is converted to kinetic

energy of implosion. They have been studied in solid targets at laser wavelengths of 0.53,¹ 1.06,¹⁻⁴ and 10.6 μ m,^{5,6} and in gas targets at 10.6 μ m.⁷ The generation of fast electrons is usually associated with resonance absorption^{1,7} but two-plasmon decay and stimulated Raman scattering (SRS)⁸ are also believed to be important production mechanisms.

In an extension of a previous experiment,⁹ we have studied the interaction of intense laser light with a gas jet. In contrast to all previous experiments with intensities greater than 10^{15} W/cm²